Multichannel Interference in Resonancelike Enhancement of High-Order Above-Threshold Ionization

Long Xu and Libin Fu*
Graduate School of China Academy of Engineering Physics, No. 10 Xibeiwang East Road, Haidian District, Beijing, 100193, China

(Received 27 November 2018; revised manuscript received 21 March 2019; published 26 June 2019)

The intensity-dependent resonancelike enhancement phenomenon in the high-order above-threshold ionization spectrum is a typical quantum effect for atoms or molecules in an intense laser field, which has not been well understood. The calculations of the time-dependent Schrödinger equation (TDSE) are in remarkable agreement with the experimental data, but they cannot clarify the contributions of the bound states. The semiclassical approach of strong field approximation, in which no excited states are involved, can obtain a similar phenomenon, but the laser intensities of enhanced regions predicted by the strong field approximation are inconsistent with the results of the TDSE. In this Letter, a new fully quantum model is established from the TDSE without any excited states. Two types of enhanced structures, unimodal and multimodal structures, are found in the results of the TDSE and model. In addition, the calculations of the model reproduce the key features of the results of the TDSE. It shows that the excited states are not the key factor in the resonancelike enhancements in our calculated system, since there are no excited states in our model. Based on the calculations of our model, we show that such resonancelike enhancements are caused by the constructive interference of different momentum transfer channels. Last, the Fano-like line shapes are also discussed for the features of multichannel interference.

DOI: 10.1103/PhysRevLett.122.253202

Above-threshold ionization (ATI) is the most fundamental and essential nonperturbative phenomenon in the interaction of an intense laser pulse with atoms or molecules, and it has attracted extensive attention [1–3] due to various possible applications since it was first observed 40 years ago [4]. ATI reveals that the electron can absorb more photons than required to exceed the ionization threshold for atoms or molecules in the intense laser field. The ATI spectra have been well understood by combining the contributions of direct ionization and the rescattering process. For an electron kinetic energy less than $2U_p$, the ATI spectrum decreases exponentially, where $2U_p$ is the maximal energy of a directly ionized electron [5–7] and $U_p = E_0^2/(4\omega^2)$ is the ponderomotive energy. E_0 and ω are the laser peak intensity and laser frequency, respectively. The high-energy spectrum appears as a flat plateau extending to $10U_p$ [6–8], which originates from the elastic scattering of electron when it revisits the parent ion.

In addition to the aforementioned features, an intensity-dependent enhancement phenomenon in high-order ATI spectrum, the so-called resonancelike enhancements (RLEs), was discovered in the rare gases xenon [9] and argon [10] two decades ago, triggering great interest both experimentally and theoretically. In 2003, Grasbon *et al.* [11] discovered that RLEs are pronounced in multicycle laser pulses and are suppressed in few-cycle pulses. Recently, the RLEs were also observed experimentally in the molecular system including H_2 [12], N_2 [13], formic acid [14], and the polyatomic molecules C_2H_4 and C_2H_6 [15]. RLEs are very sensitive to the laser intensity, and only a few percent increase in the laser intensity will result in the ATI peaks on the plateau being enhanced by up to an order of magnitude. In the past two decades, great efforts have been made to study the underlying mechanism, but no consensus has yet been reached.

RLEs are indeed the quantum effects of atoms or molecules in the intense laser field and cannot be described by the classical (semiclassical) three-step model [8], although it has successfully explained the main features of the ATI spectrum. The theoretical calculations of the time-dependent Schrödinger equation (TDSE) in the single active electron approximation are in remarkable agreement with the experimental data, indicating that high-order ATI can be explained by single electron dynamics [16]. The interpretations based on the results of the TDSE [17–19] and the Floquet approach [19–22] suggest that the RLE structures are attributed to multiphoton resonance with laser-dressed excited states, analogous to the Freeman resonances at low intensities [23].

Further theoretical research based on the strong field approximation (SFA) obtain similar enhanced structures without considering excited states [24–31]. The explanations of the SFA argue that the kinetic energy of an ejected electron in ATI is $\varepsilon_n = n\omega - I_p - U_p$, where I_p is the ionization potential. Hence, when $m\omega = I_p + U_p$, there are many electrons released with near-zero kinetic energies that

will be driven by the multicycle laser field into recollisions with the parent ion many times, and the constructive interference of a multitude of such trajectories will result in the RLEs.

The semiclassical interpretations based on the SFA grasp the main features that RLEs result from constructive interference of rescattering trajectories. However, although the SFA can give similar enhanced structures, the location and amplitude of the enhanced structures are different from those of the TDSE. Additionally, Kopold *et al.* [26] have shown that the SFA can only get a partial qualitative result compared with the experiment.

Therefore, to better understand RLEs and clarify the contribution of excited and continuum states to RLEs, a new fully quantum model is established from the TDSE without any excited states in this Letter. In the calculations of the TDSE and model, two types of enhanced structures, unimodal and multimodal structures, are observed. Based on the calculations of the model, we know the RLEs are due to the constructive interference of different momentum transfer channels caused by the combination of the laser field and the ionic potential. For the features of multichannel interference, the Fano-like line shapes are also discussed in the end.

We start with the TDSE in the single active electron approximation, and the Hamiltonian within the length gauge reads

$$\begin{aligned} H(t) &= -\frac{1}{2}\frac{\partial^2}{\partial x^2} + V(x) + W(x,t) \\ &= H_a + W(x,t) = H_V + V(x), \end{aligned} \tag{1}$$

where $V(x) = -1/\sqrt{x^2+a^2}$ represents the soft-core electron-nucleus interaction [32,33], with the soft-core parameter being $a^2 = 0.484$ to match the first ionization energy of the helium atom. $W(x,t) = xE(t)$ denotes the atom-field interaction. H_a and H_V stand for the atomic Hamiltonian and the Hamiltonian of a free electron in an external field, respectively.

The wave functions of bound states (i.e., the functions whose corresponding eigenvalues are negative among the eigenfunctions of H_a) and the Volkov functions $\psi_p(x,t) = (2\pi)^{-1/2}\exp\{i[p+A(t)]x - i\int^t [p+A(\tau)]^2/2d\tau\}$ can be used to construct an overcomplete basis of the Hilbert space. Then, we expand the wave function by using the overcomplete basis,

$$\Phi(x,t) = \sum_n c_n(t)\varphi_n(x,t) + \sum_p a_p(t)\psi_p(x,t), \tag{2}$$

in which $\varphi_n(x,t) = \varphi_n(x)e^{-iE_n t}$, while $\varphi_n(x)$ is the wave function of nth bound state of H_a, and E_n is the corresponding eigenenergy.

Substituting the expansion (2) into the Schrödinger equation, multiplying the conjugate of the basis functions $\psi_q^\dagger(x,t)$ and $\varphi_m^\dagger(x,t)$, and assuming that the populations of all the excited states are negligible, we can get

$$i\frac{\partial}{\partial t}a_q(t) = \sum_p a_p(t)(V_{qp} - \Lambda_{qg}V_{gp}) + c_g(t)W_{qg}, \tag{3}$$

$$i\frac{\partial}{\partial t}c_g(t) = \sum_p a_p(t)V_{gp}, \tag{4}$$

where the matrix elements of the electron-nucleus interaction are $V_{qp} = \int \psi_q^\dagger(x,t)V(x)\psi_p(x,t)dx$ and $V_{gp} = \int \varphi_g^\dagger(x,t)V(x)\psi_p(x,t)dx$, and the matrix elements of atom-field interaction are $W_{qg} = \int \psi_q^\dagger(x,t)W(x,t)\varphi_g(x,t)dx$. The term $\Lambda_{qg} = \int \psi_q^\dagger(x,t)\varphi_g(x,t)dx$ is caused by the overcomplete basis.

Furthermore, the infinite summation of momentum should be truncated in practice, so Eqs. (3) and (4) are changed into

$$i\frac{\partial}{\partial t}a_q(t) = \sum_p a_p(t)V_{qp}^* + c_g(t)W_{qg}, \tag{5}$$

$$i\frac{\partial}{\partial t}c_g(t) = \sum_p a_p(t)V_{gp}^*, \tag{6}$$

where $V_{qp}^* = V_{qp}f(p,t) - \Lambda_{qg}V_{gp}g(p,t)$, $V_{gp}^* = V_{gp}g(p,t)$. The truncation functions $f(p,t)$ and $g(p,t)$ are chosen as

$$f(p,t) = \begin{cases} 1, & \text{if } [p+A(t)]^2 \le 2B[B = 3.17U_p], \\ \exp[-b(|p+A(t)| - \sqrt{2B})^2], & \text{otherwise}, \end{cases} \tag{7}$$

$$g(p,t) = \begin{cases} 1, & \text{if } [p+A(t)]^2 \le 2C[C = \min(I_p/2, U_p)], \\ \exp[-b(|p+A(t)| - \sqrt{2C})^2], & \text{otherwise}, \end{cases} \tag{8}$$

where we set the damping rate of the truncation functions $b = 5$. Here, the truncation function $f(p,t)$ is set by a physical consideration that the maximum energy of the returned electron is $3.17U_p$ [5,34], and the truncation energy of $g(p,t)$ is set empirically [35] by comparing with the simulations of the TDSE. Consequently, we have derived a fully quantum model [Eqs. (5) and (6)] from the TDSE without any excited states. The details on the model derivation can be found in Sec. I of the Supplemental Material [35].

We use the fourth-order Runge-Kutta algorithm and the split-operator method [36] to numerically solve the model and TDSE, respectively. The initial state, ground state, is obtained by applying the imaginary-time propagation. A time step of 0.05 a.u. and 16 384 grid points with a spatial step of 0.25 a.u. are used.

In our calculations, we use 800 nm laser pulses with a total duration of 16 optical cycles, switched on and off linearly over two cycles. To observe the RLEs, we scan the laser intensity from 1.5 to 2.5×10^{14} W/cm^2 and plot the energy spectra in Fig. 1. All the results calculated by the TDSE, SFA [37–39], and our model show the pronounced RLEs. The enhanced regions are irregularly located around some intensities for the calculations of the one-dimensional TDSE [Fig. 1(a)]. This phenomenon that the enhanced regions are not related to $(I_p + U_p)/\omega$ can also be found in the energy spectra of xenon calculated by the three-dimensional TDSE [40]. However, the enhancements are always pronounced at integer values of $(I_p + U_p)/\omega$ both in the calculations of the one-dimensional SFA [Fig. 1(b)] and three-dimensional SFA [28].

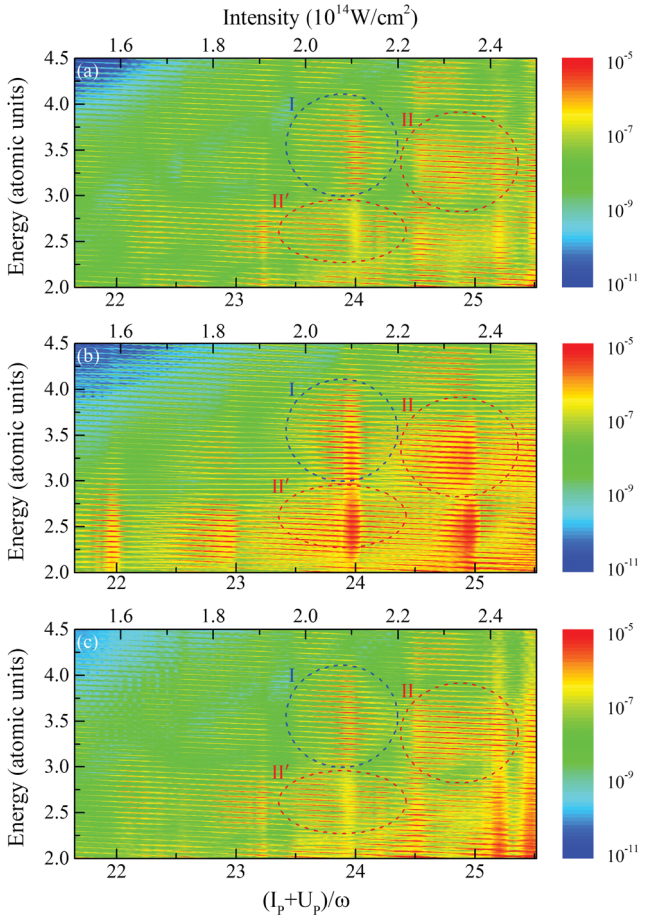

FIG. 1. Photoelectron energy spectra calculated by (a) TDSE, (b) SFA, and (c) model, as a function of the laser intensity or the parameter $(I_p + U_p)/\omega$. Three islands I, II, and II′ are marked.

The calculations of the model [Fig. 1(c)] reproduce the RLEs similar to those of the TDSE. The RLEs depend on the intensity and energy, leading to the islands in the energy spectra. There are two types of patterns for islands in the calculations of the TDSE and model. The enhanced structures in island I are pronounced in the center of the intensity of the island, while the enhancements in islands II and II′ are distributed over a wide range of the intensity.

To observe the elaborate structures, we plot the ionization rate as a function of $(I_p + U_p)/\omega$ for different ATI peaks in Fig. 2. The rate is the normalization of the summation of the probability of the energy range from $\varepsilon_n - \omega/2$ to $\varepsilon_n + \omega/2$. The orders of the ATI peaks in each island can be seen in Sec. III of the Supplemental Material [35]. As plotted in Fig. 2, the enhanced structures of different ATI peaks in each island calculated by each method are qualitatively consistent. The results of the TDSE show there are two types of enhanced structures within one order difference of $(I_p + U_p)/\omega$. The structures in island I [Fig. 2(a)] are unimodal and the structures in island II [Fig. 2(b)] are multimodal. On the contrary, the calculations of the SFA [Figs. 2(c) and 2(d)] always exhibit unimodal structures. The calculations of model are qualitatively consistent with the results of the TDSE. The enhanced structures in islands I [Fig. 2(e)] and II [Fig. 2(f)] are unimodal and multimodal, respectively. In addition, the enhanced structures in island II′ calculated by the TDSE, SFA, and model are qualitatively consistent with those in island II (see Sec. III of the Supplemental Material [35]). The agreement between the TDSE and model indicates that the excited states are not fundamental to the RLEs because

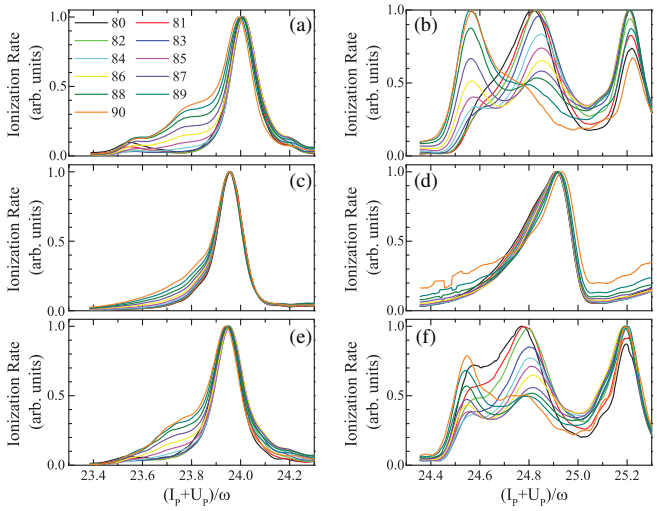

FIG. 2. (Left) Normalized differential ionization rate calculated by (a) TDSE, (c) SFA, and (e) model as a function of $(I_p + U_p)/\omega$ for island I. (Right) Normalized differential ionization rate calculated by (b) TDSE, (d) SFA, and (f) model as a function of $(I_p + U_p)/\omega$ for island II. All the orders of ATI peaks, i.e., photon numbers absorbed by electrons, for different lines are labeled in (a).

the model does not contain any excited states. The structures calculated by the SFA and TDSE or model have an evident difference, indicating that the underlying mechanisms of RLEs should be further studied.

To clarify the mechanisms of RLEs, we analyze the three processes in the model (also see Sec. IV of the Supplemental Material [35]). The first process is W_{pg}, the direct ionization process from the ground state. Another is V^*_{qp}, the transfer process between the continuum states. The third is V^*_{gp}, the recombination of the electron from the continuum state into the ground state. After assuming $c_g(t) = 1$, we can write

$$i\frac{\partial}{\partial t}a_q(t) = \sum_p a_p(t)V^*_{qp} + W_{qg}. \tag{9}$$

As plotted in Fig. 3(a), the energy spectra calculated by Eq. (9) also reproduce the enhanced structures, which are similar to the results of the TDSE and model. This reveals that the dynamics of the ground state is not the key factor in the RLEs.

Next, we separately fix the laser intensities of one of the two processes, namely, W_{pg} and V^*_{qp}, and investigate the intensity-dependent effect of the other process. In Fig. 3(b), we fix the laser intensity of W_{pg} to 2×10^{14} W/cm^2 and scan the intensity of the transfer process. There are still resonance patterns in the energy spectra, indicating that the direct ionization process is not the key factor in the RLEs. Additionally, the electron liberated with finite kinetic energy (even greater than one photon energy) during the direct ionization process contributes significantly to RLEs (see Sec. V of the Supplemental Material [35]). On the contrary, in Fig. 3(c), we keep the laser intensity of V^*_{qp} at 2×10^{14} W/cm^2 and scan the intensity of W_{pg}. The enhanced structures disappear in the energy spectra, indicating that the RLEs are mainly caused by the interference of momentum transfer processes. Different momenta may transfer to the same final momentum, and each transfer channel has a different phase. As the intensity increases, the phase changes accordingly. For some intensities, the constructive interferences occur and lead to the RLEs.

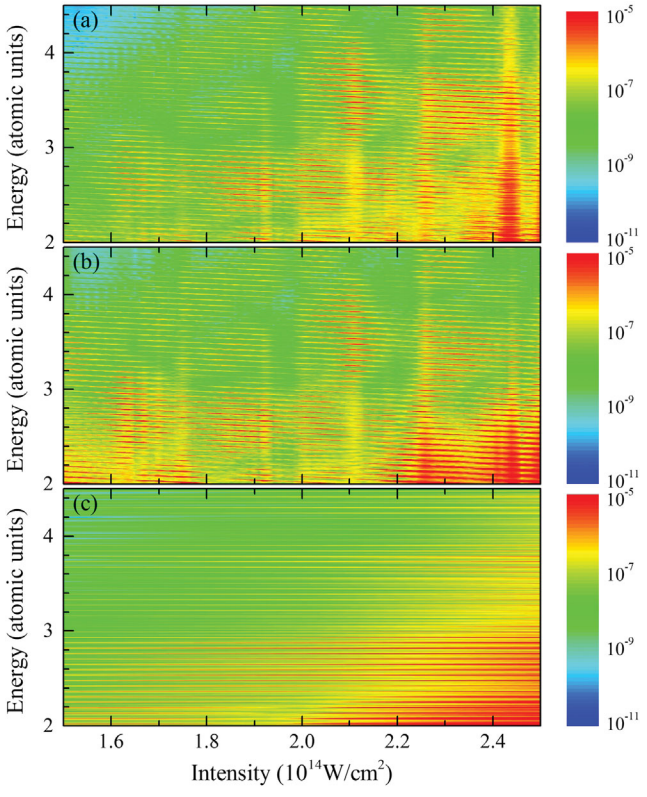

FIG. 3. Photoelectron energy spectra calculated by (a) Eq. (9), (b) Eq. (9) with the intensity of W_{pg} kept as 2×10^{14} W/cm^2, and (c) Eq. (9) with the intensity of V^*_{qp} kept as 2×10^{14} W/cm^2.

To further explore the effect of the direct ionization on the enhanced structures, we plot the differential ionization rate, which is the summation of the probability of energy range from $\varepsilon_n - \omega/2$ to $\varepsilon_n + \omega/2$, as a function of the laser intensity in Fig. 4(a). Here the solid lines present the case of Fig. 1(c) and the dotted lines present the case of Fig. 3(b). Their oscillating structures varying with the intensity are similar. The difference in amplitudes reveals that direct ionization is not negligible in the ionization rate. For the scanned intensity less than the fixed intensity (2×10^{14} W/cm^2), the ionization rate is overestimated. When the scanned intensity is greater than the fixed intensity, the rate is underestimated in most cases.

To our knowledge, such resonant structure caused by the multichannel interference may have the shape of Fano resonance and its line shape can be fitted by the Fano formula [41]

$$R = R_b\frac{(\epsilon + q)^2}{\epsilon^2 + 1}, \tag{10}$$

where $\epsilon = 2(\varepsilon - \varepsilon_r)/\Gamma_\varepsilon = 2(I_0 - I_r)/\Gamma$ is the reduced energy with the resonance width $\Gamma = 4\omega^2\Gamma_\varepsilon$ by using the relation $\varepsilon = n\omega - I_p - U_p$, R_b is the smoothly varying background parameter, q is the Fano asymmetry parameter, $I_0 = E_0^2$, and I_r is the resonant position. We choose the isolated unimodal structures marked in Fig. 4(a) [also seen in Fig. 2(e)] to study the Fano resonance and the contribution of direct ionization. We use the Fano formula (10) to fit the isolated unimodal structures. All the coefficients of determination R^2 are greater than 0.995, indicating that the fitting results can well reproduce the calculated curves. Taking the photon number $n = 85$ as a sample, we plot the calculated and fitting results in Fig. 4(b). The fitting parameters I_r, Γ, R_b, and q are displayed in Figs. 4(c)–4(f). The four fitting parameters varying with the photon numbers in the two cases are closely similar. As photon numbers increase, the resonant position I_r varies slightly and the resonance width Γ increases slowly

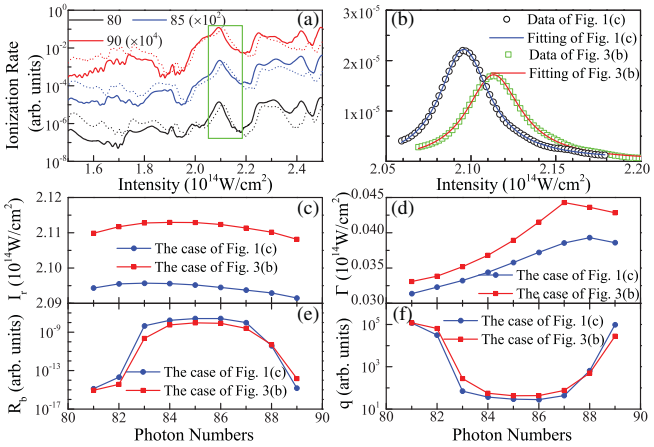

FIG. 4. (a) Differential ionization rate as a function of the laser intensity for the case of Fig. 1(c) (solid lines) and Fig. 3(b) (dotted lines) with photon numbers absorbed by electrons $n = 80$, 85, and 90, where the results of different n are multiplied by different multiples to facilitate separation. (b) The data and the fitting result as a function of the laser intensity for photon numbers $n = 85$. The fitting parameters (c) I_r, (d) Γ, (e) R_b, and (f) q as a function of photon numbers.

between 3 and 4.5×10^{12} W/cm^2. The different values in the two cases show that the direct ionization affects the resonant position and resonance width. Figures 4(e) and 4(f) show that the trends of R_b and q in both cases are basically the same, where they vary slightly around $n = 85$ but change rapidly at $n = 82$ and 88. This means that, for the selected region of RLEs, the ATI peak near the 85th order is the center of resonance and the ATI peaks around the 82nd and 88th orders are critical regions. Hence, we have studied the enhanced structures from two dimensions of laser intensity and ATI peak by using the Fano formula. There are resonance centers and resonance widths in both dimensions. Moreover, the direct ionization affects the position, width, and magnitude of the enhanced structures, although it is not the key factor in the RLEs.

In addition, the fitting structures tend to the Lorentzian profiles $R = R_b'(\Gamma/4)/[(I_0 - I_r)^2 + (\Gamma/2)^2]$, due to the parameter q being large. For the Lorentzian profiles, the line width depends on the lifetime of the energy levels and the collision broadening [42]. In the calculation, we do not consider any decay of all the states because the excited states are not taken into account in the model. Hence, the line width is caused by the collision broadening and the average collision interval $\tau_{\text{coll}} = 1/(\pi\Gamma_\varepsilon)$ between electron and ion is in the range of $T/2.29$ to $T/3.43$, where T is the laser period.

In summary, we have derived a new quantum model without excited states from the TDSE. We have observed that the differential ionization rate of each ATI peak as a function of the laser intensity has two types of enhanced structures in the calculations of the TDSE and our model. One is the same unimodal structure at the integer values of $(I_p + U_p)/\omega$ as the calculation of the SFA, the other is a multimodal structure within one order difference of $(I_p + U_p)/\omega$. Based on the calculations of our model, we show that the constructive interference of different momentum transfer channels, rather than the excited states, lead to the RLEs. Additionally, the direct ionization affects the position, width, and magnitude of the enhanced structures. Finally, the Fano-like line shapes are studied to explore the dependence of RLEs on the laser intensity and the ATI peak and to confirm the contributions of the transfer and the direct ionization processes. We hope that the abundant structures, such as the unimodal or multimodal enhanced structures and the Fano line shapes, will be observed in experiments in the future.

This work was supported by National Natural Science Foundation of China (Grants No. 11725417, No. 11575027), NSAF (Grant No. U1730449), and Science Challenge Project (Grant No. 2018005).

*lbfu@gscaep.ac.cn

[1] W. Becker, X. J. Liu, P. J. Ho, and J. H. Eberly, Theories of photoelectron correlation in laser-driven multiple atomic ionization, Rev. Mod. Phys. **84**, 1011 (2012).
[2] R. Pazourek, S. Nagele, and J. Burgdörfer, Attosecond chronoscopy of photoemission, Rev. Mod. Phys. **87**, 765 (2015).
[3] L. Y. Peng, W. C. Jiang, J. W. Geng, W. H. Xiong, and Q. H. Gong, Tracing and controlling electronic dynamics in atoms and molecules by attosecond pulses, Phys. Rep. **575**, 1 (2015).
[4] P. Agostini, F. Fabre, G. Mainfray, G. Petite, and N. K. Rahman, Free-Free Transitions Following Six-Photon Ionization of Xenon Atoms, Phys. Rev. Lett. **42**, 1127 (1979).
[5] G. G. Paulus, W. Becker, W. Nicklich, and H. Walther, Rescattering Effects in Above-Threshold Ionization: A Classical Model, J. Phys. B **27**, L703 (1994).
[6] G. G. Paulus, W. Nicklich, H. Xu, P. Lambropoulos, and H. Walther, Plateau in Above Threshold Ionization Spectra, Phys. Rev. Lett. **72**, 2851 (1994).
[7] W. Becker, F. Grasbon, R. Kopold, D. B. Milošević, G. G. Paulus, and H. Walther, Above-threshold ionization: from classical features to quantum effects, Adv. At. Mol. Opt. Phys. **48**, 35 (2002).
[8] P. B. Corkum, Plasma Perspective on Strong Field Multiphoton Ionization, Phys. Rev. Lett. **71**, 1994 (1993).
[9] P. Hansch, M. A. Walker, and L. D. Van Woerkom, Resonant hot-electron production in above-threshold ionization, Phys. Rev. A **55**, R2535 (1997).
[10] M. P. Hertlein, P. H. Bucksbaum, and H. G. Muller, Evidence for resonant effects in high-order ATI spectra, J. Phys. B **30**, L197 (1997).
[11] F. Grasbon, G. G. Paulus, H. Walther, P. Villoresi, G. Sansone, S. Stagira, M. Nisoli, and S. De Silvestri, Above-Threshold Ionization at the Few-Cycle Limit, Phys. Rev. Lett. **91**, 173003 (2003).

[12] C. Cornaggia, Enhancements of rescattered electron yields in above-threshold ionization of molecules, Phys. Rev. A **82**, 053410 (2010).
[13] W. Quan, X. Y. Lai, Y. J. Chen, C. L. Wang, Z. L. Hu, X. J. Liu, X. L. Hao, J. Chen, E. Hasović, M. Busuladžić, W. Becker, and D. B. Milošević, Resonancelike enhancement in high-order above-threshold ionization of molecules, Phys. Rev. A **88**, 021401(R) (2013).
[14] C. Wang, Y. Tian, S. Luo, W. G. Roeterdink, Y. Yang, D. Ding, M. Okunishi, G. Prümper, K. Shimada, K. Ueda, and R. Zhu, Resonance-like enhancement in high-order above-threshold ionization of formic acid, Phys. Rev. A **90**, 023405 (2014).
[15] C. Wang, M. Okunishi, X. Hao, Y. Ito, J. Chen, Y. Yang, R. R. Lucchese, M. Zhang, B. Yan, W. D. Li, D. Ding, and K. Ueda, Resonancelike enhancement in high-order above-threshold ionization of polyatomic molecules, Phys. Rev. A **93**, 043422 (2016).
[16] M. J. Nandor, M. A. Walker, L. D. Van Woerkom, and H. G. Muller, Detailed comparison of above-threshold-ionization spectra from accurate numerical integrations and high-resolution measurements, Phys. Rev. A **60**, R1771 (1999).
[17] H. G. Muller and F. C. Kooiman, Bunching and Focusing of Tunneling Wave Packets in Enhancement of High-Order Above-Threshold Ionization, Phys. Rev. Lett. **81**, 1207 (1998).
[18] H. G. Muller, Numerical simulation of high-order above-threshold-ionization enhancement in argon, Phys. Rev. A **60**, 1341 (1999).
[19] J. Wassaf, V. Véniard, R. Taïeb, and A. Maquet, Roles of resonances and recollisions in strong-field atomic phenomena: above-threshold ionization, Phys. Rev. A **67**, 053405 (2003).
[20] J. Wassaf, V. Véniard, R. Taïeb, and A. Maquet, Strong Field Atomic Ionization: Origin of High-Energy Structures in Photoelectron Spectra, Phys. Rev. Lett. **90**, 013003 (2003).
[21] R. M. Potvliege and S. Vučić, High-order above-threshold ionization of argon: plateau resonances and the Floquet quasienergy spectrum, Phys. Rev. A **74**, 023412 (2006).
[22] R. M. Potvliege and S. Vučić, Freeman resonances in high-order above-threshold ionization, J. Phys. B **42**, 055603 (2009).
[23] R. R. Freeman, P. H. Bucksbaum, H. Milchberg, S. Darack, D. Schumacher, and M. E. Geusic, Above-Threshold Ionization with Subpicosecond Laser Pulses, Phys. Rev. Lett. **59**, 1092 (1987).
[24] R. Kopold and W. Becker, Interference in high-order above-threshold ionization, J. Phys. B **32**, L419 (1999).
[25] G. G. Paulus, F. Grasbon, H. Walther, R. Kopold, and W. Becker, Channel-closing-induced resonances in the above-threshold ionization plateau, Phys. Rev. A **64**, 021401(R) (2001).
[26] R. Kopold, W. Becker, M. Kleber, and G. G. Paulus, Channel-closing effects in high-order above-threshold ionization and high-order harmonic generation, J. Phys. B **35**, 217 (2002).
[27] S. V. Popruzhenko, P. A. Korneev, S. P. Goreslavski, and W. Becker, Laser-Induced Recollision Phenomena: Interference Resonances at Channel Closings, Phys. Rev. Lett. **89**, 023001 (2002).
[28] D. B. Milošević, E. Hasović, M. Busuladžić, A. Gazibegović-Busuladžić, and W. Becker, Intensity-dependent enhancements in high-order above-threshold ionization, Phys. Rev. A **76**, 053410 (2007).
[29] D. B. Milošević, E. Hasović, S. Odžak, M. Busuladžić, A. Gazibegović-Busuladžić, and W. Becker, Wavelength dependence of channel-closing enhancements in high-order above-threshold ionization and harmonic generation, J. Mod. Opt. **55**, 2653 (2008).
[30] D. B. Milošević, W. Becker, M. Okunishi, G. Prümper, K. Shimada, and K. Ueda, Strong-field electron spectra of rare-gas atoms in the rescattering regime: enhanced spectral regions and a simulation of the experiment, J. Phys. B **43**, 015401 (2010).
[31] X. Y. Lai, C. L. Wang, Y. J. Chen, Z. L. Hu, W. Quan, X. J. Liu, J. Chen, Y. Cheng, Z. Z. Xu, and W. Becker, Elliptical Polarization Favors Long Quantum Orbits in High-Order Above-Threshold Ionization of Noble Gases, Phys. Rev. Lett. **110**, 043002 (2013).
[32] J. Javanainen, J. H. Eberly, and Q. Su, Numerical simulations of multiphoton ionization and above-threshold electron spectra, Phys. Rev. A **38**, 3430 (1988).
[33] Q. Su and J. H. Eberly, Model atom for multiphoton physics, Phys. Rev. A **44**, 5997 (1991).
[34] J. L. Krause, K. J. Schafer, and K. C. Kulander, High-Order Harmonic Generation from Atoms and Ions in the High Intensity Regime, Phys. Rev. Lett. **68**, 3535 (1992).
[35] See Supplemental Material at http://link.aps.org/supplemental/10.1103/PhysRevLett.122.253202 for additional details. It is divided into five sections: I. the model derivation, II. the effects of the truncation functions, III. the ATI peaks in the energy spectra, IV. the ionization diagram of the model, and V. the contribution of the directly ionized electron with finite kinetic energy.
[36] M. Feit, J. Fleck, and A. Steiger, Solution of the Schrödinger equation by a spectral method, J. Comput. Phys. **47**, 412 (1982).
[37] L. V. Keldysh, Ionization in the field of a strong electromagnetic wave, Zh. Eksp. Teor. Fiz. **47**, 1945 (1965) [Sov. Phys. JETP **20**, 1307 (1965)].
[38] F. H. M. Faisal, Multiple absorption of laser photons by atoms, J. Phys. B **6**, L89 (1973).
[39] H. R. Reiss, Effect of an intense electromagnetic field on a weakly bound system, Phys. Rev. A **22**, 1786 (1980).
[40] B. B. Li, S. L. Hu, Z. Shu, X. T. He, and J. Chen, Resonance-like enhancement in high-order above threshold ionization of atoms and molecules in intense laser fields, Opt. Express **26**, 13012 (2018).
[41] U. Fano, Effects of configuration interaction on intensities and phase shifts, Phys. Rev. **124**, 1866 (1961).
[42] R. Loudon, *The Quantum Theory of Light* (Oxford University Press, Oxford, 2000).